Shahid Bahonar University of Kerman

Biomechanism and Bioenergy Research

Online ISSN: 2821-1855
Homepage: https://bbr.uk.ac.ir

Iranian Society of Agricultural Machinery Engineering and Mechanization

Prediction of Enzymatic Activity of *Aspergillus* Species Using Visible-Near Infrared Machine Vision System

Mohammad Hossein Nargesi[1], Khadijeh Abbasi[2]✉, Zeinab Bastami[2], Kamran Kheiralipour[1]

[1] Mechanical Engineering of Biosystems Department, Ilam University, Ilam, Iran.
[2] Plant Protection Department, Ilam University, Ilam, Iran.
✉ Corresponding author: kh.abasi@ilam.ac.ir

ARTICLE INFO

Article type:

Research Article

Article history:

Received 11 November 2025

Received in revised form 28 December 2025

Accepted 21 February 2026

Available Online 31 March 2026

Keywords:

Chitinase enzyme, Fungal isolates, Hyperspectral imaging, Image processing.

ABSTRACT

Various species of the filamentous fungus Aspergillus are among the most common fungi found in air, soil, plants, and indoor environments. Many species of this genus are of significant importance in economic, biotechnological, and medical contexts, particularly in the production of enzymes, organic acids, antibiotics, and other bioactive metabolites. However, some species are opportunistic pathogens capable of causing diseases in both plants and humans. Hyperspectral imaging is a useful tool for identifying fungal traits, and when combined with machine learning, it enables more accurate and automated detection. In this study, the effect of time on the fungal growth and production of chitinase enzyme in Aspergillus endophytic isolates was investigated and a comparison was made between the isolates. The results showed that with time, the enzymatic activity of the fungal isolates increased. Additionally, significant differences were observed between the fungal isolates. The fungal growth increased with increasing enzyme activity duration too.

Cite this article: Nargesi, M. H., Abbasi, Kh., Bastami, Z., & Kheiralipour, K (2026). Prediction of Enzymatic Activity of Aspergillus Species Using Visible-Near Ingfrared Machine Vision System. *Biomechanism and Bioenergy Research*, *5*(1), 70-81. https://doi.org/10.22103/bbr.2026.26809.1146

Publisher: Shahid Bahonar University of Kerman
DOI: https://doi.org/10.22103/bbr.2026.26809.1146

INTRODUCTION

Aspergillus include a large group of fungal species that have diverse morphological, physiological, and phylogenetic characteristics and significantly affect food production and human health (Latge & Chamilos, 2019). Phylogenetic analysis and examination of various genome regions (TEF, RPB1, RPB2, 5.8S, LSU, SSU) place this genus within the phylum *Ascomycota*, class *Eurotiomycetes*, order *Eurotiales*, and family *Aspergillaceae*. According to the latest classification, the genus *Aspergillus* comprises 446 species, six subgenera, and 27 sections (Mageswari et al., 2023; Hickey et al., 2004; Hickey & Read, 2009). The varoius species of this genus have been used to produce food enzymes for more than 50 years. Cultivation methods, phenotypic detection, and studies involving various fungal species in researches are typically conducted manually and in vitro. These approaches are often inefficient, reliant on skilled experts, and both time-consuming and labor-intensive (Watt et al., 2020; Tao et al., 2022). To address these challenges, imaging technology has garnered increasing attention from researchers. Imaging technology has found extensive applications across various agricultural fields, including food and agricultural evaluations (Kheiralipour and kazemi, 2019; Khazaei et al., 2022; Hossainpour et al., 2023; Nargesi and Kheiralipour, 2024; Farrokhzad et al., 2024; Ilgoth et al., 2024; Kheiralipour, 2024). HSI techniques have been applied in various industries (Vadivambal and Jayas, 2016; Kheiralipour and Jayas, 2023c; Kheiralipour and Jayas, 2024a; Nargesi et al., 2024a).

The aim of this study is to investigate the effect of time on fungal growth and chitinase enzyme production in Aspergillus endophytic isolates using hyperspectral imaging technology, an innovative approach that has not yet been used in this field. Also, in this study, fungal growth days were separated using HSI.

MATERIALS AND METHODS

Collecting Plant Samples

The fungal isolates belonging to the genus *Aspergillus* were sourced from the living plant fungi collection at the Faculty of Agriculture, Ilam University, Ilam, Iran. Various culture media, including water agar, potato dextrose agar, potato carrot agar, Czapek-Dox agar, malt extract agar, and yeast extract agar were used for identification and identification of fungal species. Two methods of single spore and hyphal tip were used to purify the isolates.

Chitinase Enzyme Activity Assay

Colloidal chitin was used as a substrate for preparing a culture medium to induce chitinase enzyme production. To prepare colloidal chitin, 10 g of chitin powder were mixed with 100 ml of 85% phosphoric acid, and the mixture was stored at 4°C for 24 h. Water was then added to the mixture, and the resulting solution was filtered using filter paper. To completely remove the acid, the steps of adding water and filtering were repeated several times. The obtained paste was dried and ground into powder, which was then used as a carbon source in the water agar (WA) medium.

For preparing the basal medium for chitinase production, 5 mm discs from five-day-old isolates were cultured in MSM liquid medium containing the following components: (NH4)2SO4(NH_4)_2SO_4(NH4)2SO4: 2.8 g, urea: 0.6 g, KH2PO4KH_2PO_4KH2PO4: 4 g, CaCl2.2H2OCaCl_2.2H_2OCaCl2.2H2O: 0.6 g, MgSO4MgSO_4MgSO4: 0.2 g, FeSO4.7H2OFeSO_4.7H_2OFeSO4.7H2O: 0.01 g, ZnSO4.H2OZnSO_4.H_2OZnSO4.H2O: 0.0028 g, CoCl2.6H2OCoCl_2.6H_2OCoCl2 .6H2O: 0.0032 g, and 1 g/L of colloidal chitin. A total of 100 ml of this medium was poured into 250 mL Erlenmeyer flasks and incubated for five days at 25°C with continuous shaking at 120 rpm.

To prepare the chitin solution, 0.5% colloidal chitin was dissolved in 100 ml of distilled water. Chitinase activity was determined by measuring the release of reducing sugars from colloidal

chitin using the N-acetyl-glucosamine-dinitrosalicylic acid (DNS) method as described by Monreal and Reese (1969). The reaction mixture contained 200 µl of 0.5% chitin in citrate phosphate buffer (0.05 M, pH 6.6) and 200 µl of enzyme solution, which was incubated at 37°C for 1 h. After incubation, 1 milliliter of DNS reagent was added to the reaction, and the mixture was heated in boiling water for 5 minutes. The samples were centrifuged at 6000 rpm for 5 min and the absorbance was measured at 540 nm. Measurements were taken at 24, 48, 72, and 96 h. The spectrophotometer was zeroed using a reaction mixture in which enzyme activity had been stopped in a 100 ℃ water bath.

The ability of fungal isolates to produce chitinase was evaluated in WA medium containing 0.5% colloidal chitin, where chitin served as the sole carbon source for fungal growth. A 5 mm disc from the edge of a four-day-old fungal culture was placed at the center of the Petri dish, and the dishes were incubated at 25°C for five days. After five days, the chitinase production ability of the isolates was assessed by measuring the mycelial diameter.

To induce enzyme production in the MSM culture medium, the isolates were incubated in a shakdar incubator (Model 3033, GFL) for 24 h.

Subsequently, to enhance the reaction between the enzyme and the substrate, a B-Mari device (Model W614D, Fater Electronics) was employed.

Afterward, 1 ml of dinitro salicylic acid reagent was added to the reaction mixture, which was then placed in boiling water for five minutes. The mixture was subsequently centrifuged at 6000 rpm for five minutes.

Finally, enzyme activity in the fungus was measured using a spectrophotometer (Model 6850, Jenway) at a wavelength of 540 nm.

Chitinase specific activity was determined by measuring the release of reducing saccharides from colloidal chitin by the N-acetyl-glucosamine-dinitrosalicylate method at 540 nm. Colorimetry based on image processing technique was used to discover colour changes in minimal synthetic medium for validation of chitinase activity.

Figure 1 shows the different stages of conducting the present study to determine the amount of enzyme present in fungus using the hyperspectral imaging method, from the sample preparation stage to data analysis.

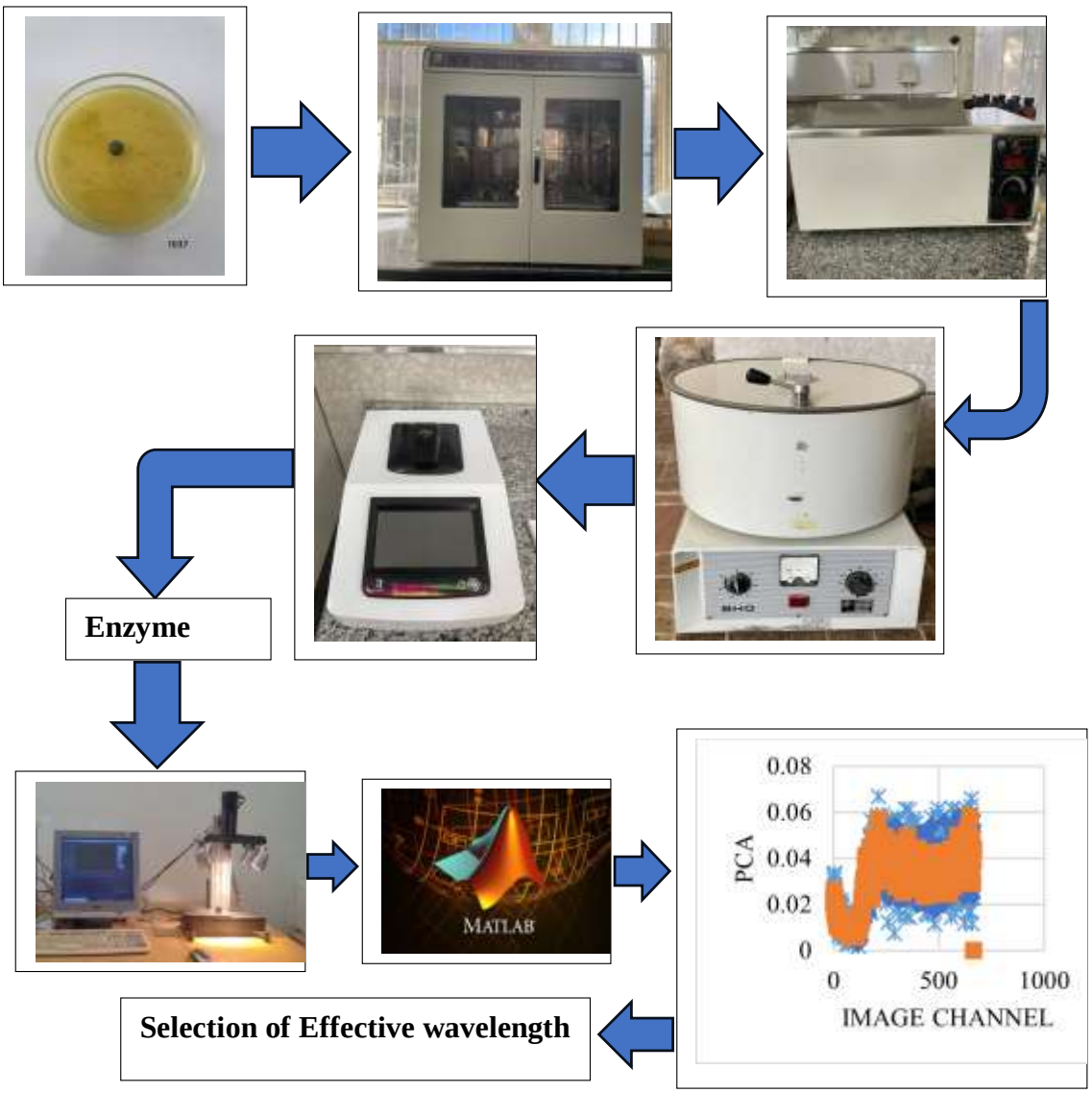

Figure 1. Different steps of enzyme determination in fungi using hyperspectral imaging.

Hyperspectral Imaging

A visible-near infrared hyperspectral imaging system (Model Specam, Parto Sanat Co., Zanjan, Iran) with a wavelength range of 400-950 nm was utilized. The imaging step was conducted at the Image Processing Laboratory, Ilam University, Ilam, Iran.

Image Processing

After recording the hyperspectral images, MATLAB software was utilized as the primary tool to process the obtained images. Initially, hyperspectral images underwent preprocessing to enhance data quality. Subsequently, efficient channels were extracted from the hyperspectral data using analytical methods. In this process, the

key wavelengths associated with the image channels were identified based on the positions of spectral peaks and selected using the principal component analysis (PCA) method. This approach enabled dimensionality reduction and focused on the most significant information, allowing for more precise identification of effective wavelengths (Nargesi et al., 2024).

RESULTS AND DISCUSSION

Identification of Fungal Isolates

Based on morphological and molecular features, the fungal isolates were classified in five species belonged to *A. candidus, A. niger, A. tubingensis, A. flavus, and A. terresu*.

Effective Wavelengths

The mean values of the principal components (PC) of hyperspectral images for all wavelengths were plotted. The PC data for all samples were presented in the form of graphs, and based on the peaks of the curves, the effective wavelengths were selected. The peaks in the graphs were identified as effective channels, and the wavelengths corresponding to these channels were determined based on the output of the imaging system. In the subsequent subsections, the results related to the differentiation of various fungi and the data for different days are presented.

The mean PC data for five species of fungi *A. candidus*, *A. niger*, *A. tubingensis*, *A. flavus*, and *A. terreus* across four different days were plotted (Figure 2). Based on the peaks of the curves, the effective channels of the hyperspectral images were selected. These effective channels and wavelengths are reported in Table 1.

The PC charts related to different growth stages of *A. candidus, A. niger, A. tubingensis, A. flavus*, and *A. terreus* are shown in Fig 2. In these charts, optimal channels were selected based on peak wavelengths, and the corresponding effective wavelengths were extracted. The details of these wavelengths are presented in Table 2-6.

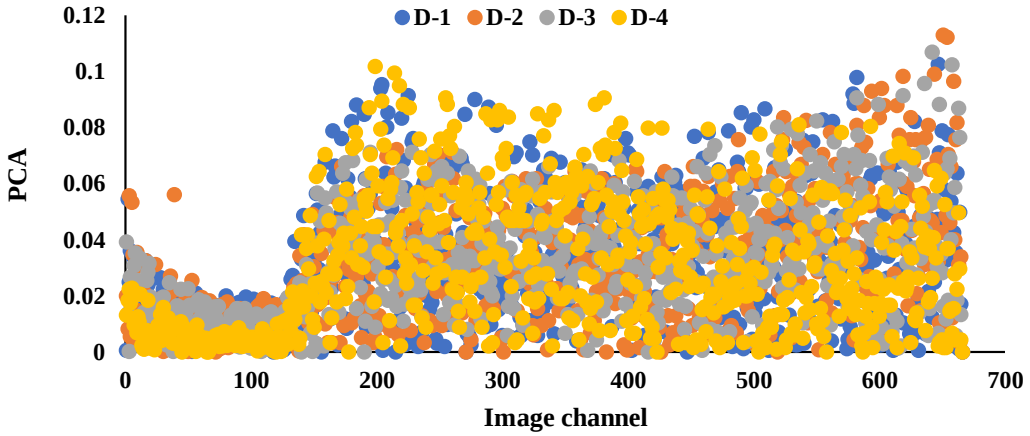

a) *Aspergillus candidus*

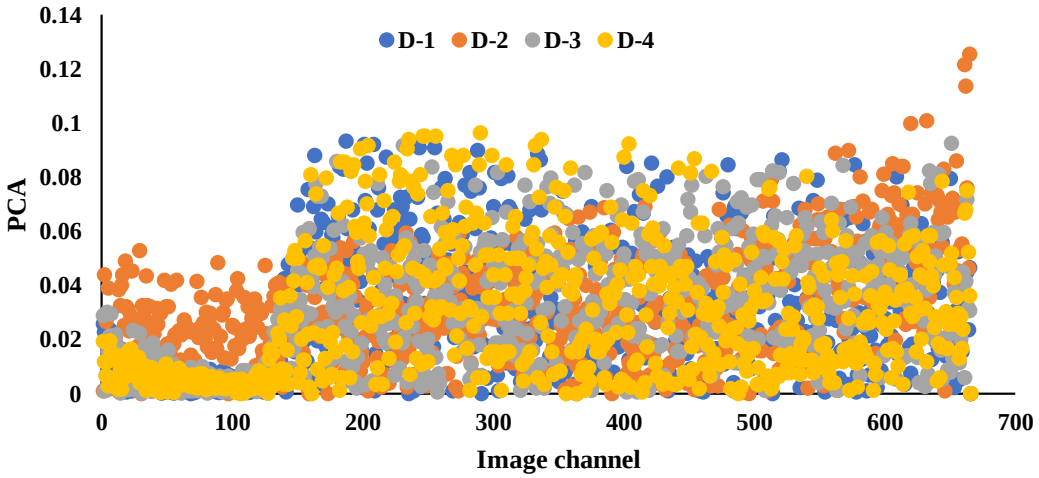

b) *Aspergillus niger*

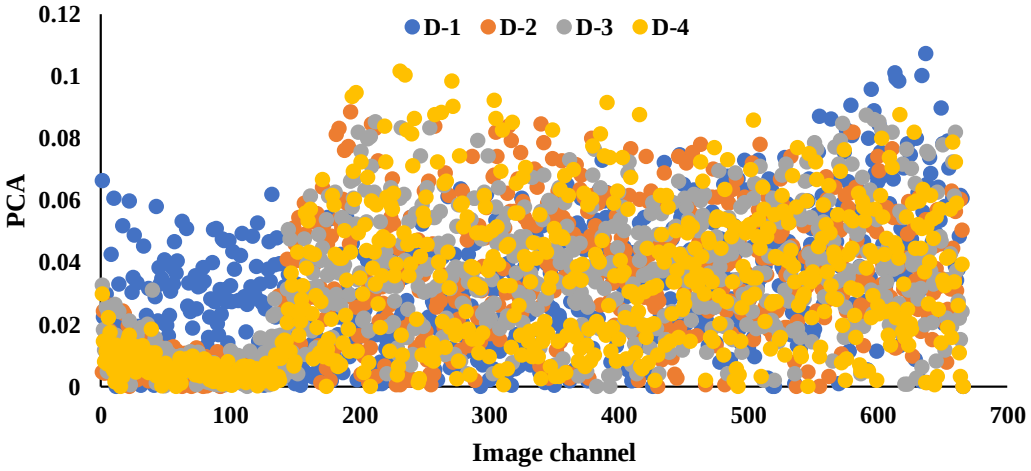

c) *Aspergillus tubingensis*

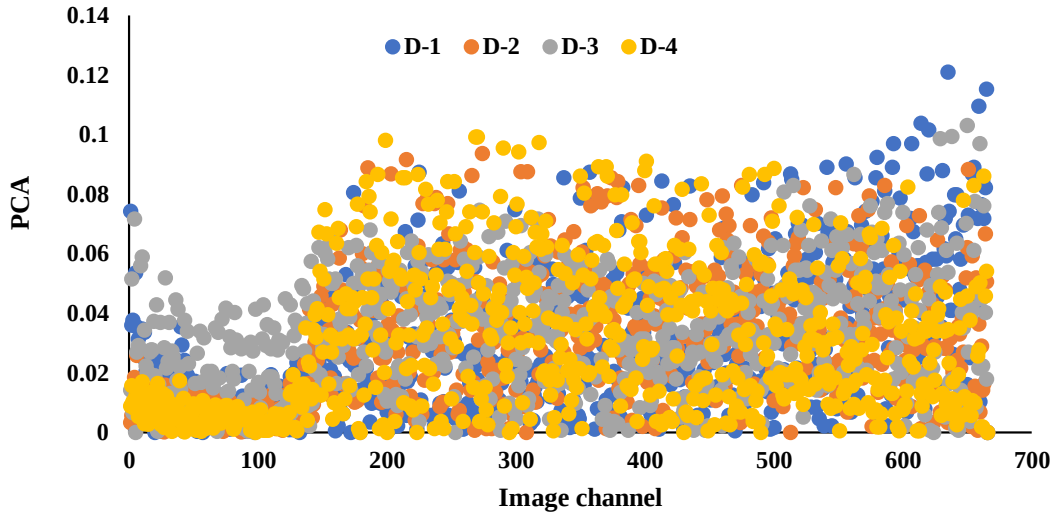

c) Aspergillus flavus

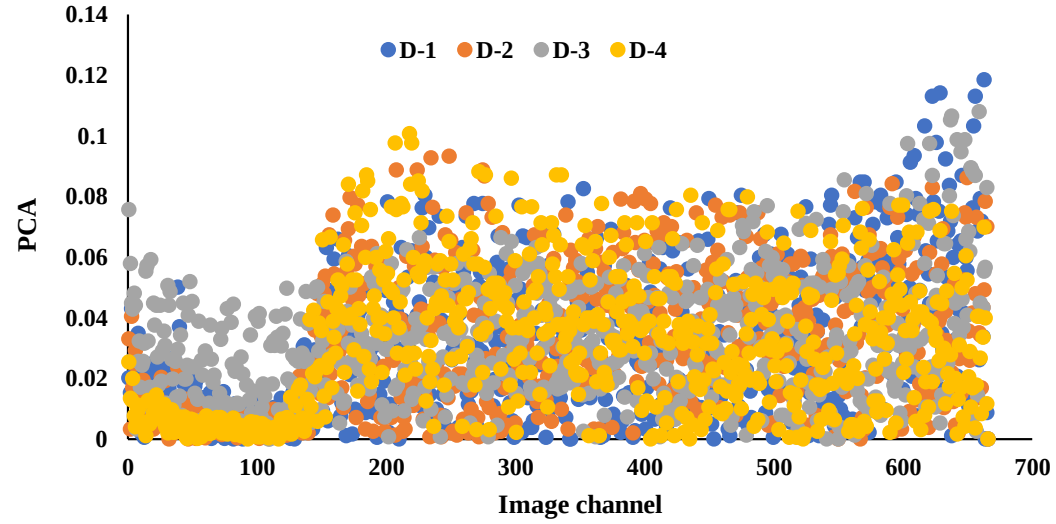

c) *Aspergillus terreus*

Figure2. *Aspergillus* fungus with different species. D-1, D-2, D-3 and D-4 represent the first day, second day, third day and fourth day for Fungal growth, respectively.

Table 1. Wavelength values for different types of fungi *A. candidus, A. niger, A. tubingensis, A. flavus, and A. terreus.*

Fungal species	Effective Channels	Effective wavelengths
A. candidus	167, 229, 289, 356, 460, 509, 525, 539, 555, 579, and 628.	537.66, 588.92, 638.53, 693.93, 779.92, 820.44, 833.67, 845.24, 858.47, 878.32, and 918.83.
A. niger	236, 288, 379, 534, 548, 592, and 624.	594.71, 637.71, 712.95, 841.11, 852.98, 889.07, and 915.52.
A. tubingensis	138, 175, 185, 378, 418, 579, 595, 612, and 637.	513.68, 544.27, 552.54, 712.12, 745.20, 878.32, 891.55, 905.60, and 926.27.
A. flavus	321, 413, 422, 487, 492, 519, 615, and 623.	664.99, 741.06, 748.50, 802.25, 806.38, 828.71, 908.08, and 914.70.
A. terreus	136, 158, 258, 259, 498, 512, 609, and 626.	512.03, 530.22, 612.90, 613.73, 811.34, 822.92, 903.12, and 917.18.

Fungal Growth

As shown in Table 2, the effective wavelength values for *A. candidus* varied over four consecutive days. The highest and lowest values for each day were observed for 693.93 638.92, and 878.32 nm wavelengths, respectively. The average values of the effective wavelengths demonstrated a decreasing trend during 1 to 4-day period. These changes reflect the sensitivity of these wavelengths in distinguishing different stages of *A. candidus* over time. Therefore, it can be concluded that these wavelengths are suitable markers for analyzing fungal growth across different days. The results showed that with increasing chitinase activity, fungal growth also increased. Image processing technique for colorimetry of the samples confirmed the results of chitinase activity. This means that increase of chitinase activity causes darkening of enzyme solution colour.

Table 2. The mean feature value corresponding the effective wavelengths for *A. candidus* in four days.

Wavelength (nm)	Day 1	Day 2	Day 3	Day 4
537.66	0.066324	0.055185	0.037104	0.027927
588.92	0.076174	0.042584	0.02152	0.016756
638.92	0.087338	0.042584	0.032652	0.002234
693.93	0.059757	0.047798	0.027457	0.011171
779.92	0.068951	0.057358	0.034136	0.024576
820.44	0.086681	0.040846	0.025231	0.002234
833.67	0.072234	0.043453	0.019294	0.001676
845.24	0.075518	0.044322	0.010389	0.005027
858.47	0.082741	0.070394	0.054172	0.011171
878.32	0.091934	0.052144	0.037846	0.017874
918.83	0.082084	0.05562	0.037104	0.01173

As observed in, the specific activity of chitinase for *A. niger* varied across the time periods of 48, 72, 96, and 120 hours. The effective wavelengths of 594.71, 637.71, 712.95, 841.11, 852.98, 889.07, and 915.52 indicated the specific activity of the enzyme. According to Table 3, a decreasing trend in the mean values was observed over different days. With increasing time, enzyme activity and fungal isolates growth increased, resulting in a darkening solution colour. Moreover, there was a significant difference in enzyme activity across different time points.

Table 3. The mean feature value corresponding the effective wavelengths for *A. niger* in four days.

W* (nm)	d1	d2	d3	d4
594.71	0.064478	0.055836	0.046901	0.007141
637.71	0.089808	0.049412	0.024791	0.005951
712.95	0.046056	0.038542	0.026801	0.015472
841.11	0.068508	0.050401	0.048241	0.015472
852.98	0.07887	0.064236	0.051591	0.032134
889.07	0.044328	0.0336	0.028141	0.011306
915.52	0.056994	0.048424	0.034841	0.015472

*W and d indicate wavelength and day, respectively.

In the *A. tubingensis* fungal isolate, enzyme activity varied over 24-hour intervals, indicating its specific activityThe effective wavelengths of 513.68, 544.27, 552.54, 712.12, 745.20, 878.32, 891.55, 905.60, and 926.27 were selected based on spectral peaks. The mean values at these wavelengths exhibited variations, reflecting the trend of enzyme activity over time. As time progressed, increased enzyme activity led to an increasing in the intensity of the isolate solution colour, consequently lowering the mean values. The highest difference in mean values was observed at the wavelength of 878.32, highlighting its significant role in assessing enzymatic activity (Table 4). Also with increasing of the enzyme activity, the fungal isolates growth increased in culture medium.

Table 4. The mean feature value corresponding the effective wavelengths for *A. tubingensis* in four days.

W* (nm)	d1	d2	d3	d4
513.68	0.039542	0.029146	0.012387	0.002064
544.27	0.054479	0.045848	0.035786	0.012065
552.54	0.042617	0.039299	0.026151	0.006985
712.12	0.058873	0.048468	0.035098	0.008255
745.20	0.041299	0.030129	0.019957	0.005715
878.32	0.090506	0.081872	0.051614	0.031751
891.55	0.095778	0.051743	0.030968	0.022225
905.60	0.066781	0.054363	0.03785	0.024765
926.27	0.107202	0.053708	0.041291	0.00127

*W and d indicate wavelength and day, respectively.

In Table 5, related to the fungus *A. flavus*, it was observed that the greatest difference in mean values occurred at the wavelength of 741.06 between the third and fourth days. This change indicates peak enzymatic activity during this time period. At this wavelength, the mean value showed a decreasing trend, reflecting increased enzymatic activity and, consequently, an increasing in the intensity of the isolate colour. Additionally, a decreasing trend in mean values was observed at other analyzed wavelengths, but the most significant difference was at 741.06, highlighting the sensitivity of this wavelength to enzymatic activity changes over time. With increasing in the enzyme activity, the fungal isolates growth increased.

Table 5. The mean feature value corresponding the effective wavelengths for *A. flavus* in four days.

W* (nm)	d1	d2	d3	d4
664.99	0.057623	0.04647	0.035834	0.019473
741.06	0.084438	0.07543	0.050018	0.002513
748.50	0.076451	0.041082	0.023889	0.011307
802.25	0.046213	0.035695	0.023143	0.013819
806.38	0.083868	0.066001	0.044046	0.030151
828.71	0.070175	0.065328	0.034341	0.013819
908.08	0.05363	0.029633	0.014931	0.008794
914.70	0.058194	0.043103	0.02165	0.011935

W* and d indicate wavelength and day, respectively.

In the *A. terreus* fungal isolate, the effective wavelengths of 512.03, 530.22, 612.90, 613.73, 811.34, 822.92, 903.12, and 917.18 were selected based on spectral peaks. The results indicate that at these effective wavelengths, the specific activity of the chitinase enzyme varied over the time periods of 48, 72, 96, and 120 hours. Furthermore, as time progressed, enzyme activity increased, leading to a darkening solution colour. These changes highlight a significant difference in enzyme activity across different days, which may be associated with the level of enzyme production and its impact on substrate degradation (Table 6). The results showed that with increasing chitinase activity, fungal growth also increased.

Table 6. The mean feature value corresponding the effective wavelengths for *A. terreus* in four days.

W* (nm)	d1	d2	d3	d4
512.03	0.030431	0.021369	0.013809	0.006032
530.22	0.048907	0.031083	0.027617	0.016786
612.90	0.05108	0.045976	0.036165	0.027277
613.73	0.063035	0.021369	0.018411	0.004196
811.34	0.060862	0.044681	0.034193	0.029375
822.92	0.053254	0.036263	0.024987	0.000525
903.12	0.093466	0.066698	0.023672	0.013638
917.18	0.097813	0.054394	0.047344	0.032522

*W and d indicate wavelength and day, respectively.

CONCLUSIONS

In the present study, the effect of time on different fungal isolates and a comparison between various fungal isolates were investigated. The results indicate that with the passage of time, the mean values of the principal component data were decreased and enzyme activity increased. Additionally, a significant difference in enzymatic activity was observed between the different fungal isolates, highlighting the varying biological impacts of each isolate. These findings emphasize the importance of both time and isolate type in enzymatic activity and their biochemical characteristics. Use of image processing technique confirmed that there is a good relationship between enzyme activity and colour intensity of enzyme solution. The colour of solution for isolates with high enzyme activity is darker than for isolates with low enzyme activity. That with increasing the duration of enzyme activity, fungal growth increases.

The results obtained could serve as a foundation for future studies involving the use of spectroscopy in identifying and analyzing similar biological species.

ACKNOWLEDGMENT

The authors thank Mechanical Engineering of Biosystems Department, Ilam University, Ilam, Iran, due to the supports for the present study.

REFERENCES

Latge, J.P., Chamilos, G. (2019). *Aspergillus fumigatus* and *Aspergillosis* in 2019. Clin Microbiol Rev 33: e00140-18. https://doi.org/10.1128/CMR 00140-18.

Lestrade, P.P., Bentvelsen, R.G., Schauwvlieghe, A.F.A.D., Schalekamp, S., van der Velden WJFM, Kuiper EJ, van Paassen J, van der Hoven B, van der Lee HA, Melchers WJG, de Haan AF, van der Hoeven HL, Rijnders BJA, van der Beek MT, Verweij PE. (2019). Voriconazole resistance and mortality in invasive aspergillosis: a multicenter retrospective cohort study. *Clin Infect Dis 68*:1463–1471.

Denning, D.W. (2024). Global incidence and mortality of severe fungal disease. Lancet Infect Dis 24: e428–e438.

Bongomin, F., Gago, S., Oladele, R.O., Denning, D.W. (2017). Global and multi-national prevalence of fungal diseases-estimate precision. J Fungi (Basel) 3:57.

Hickey, P.C., Swift, S.R., RocaMG, R. (2004). Live-cell imaging of filamentous fungi using vital fluorescent dyes and confocal microscopy. Meth Microbiol 34:63–87.

Hickey, P.C., Read, N.D. (2009). Imaging living cells of Aspergillus in vitro. Med Mycol 47: S110–S119.

Watt, M., Fiorani, F., Usadel, B., Rascher, U., Muller, O., and Schurr, U. (2020). Phenotyping: new windows into the plant for breeders. Ann. Rev. Plant Biol. 71, 689–712. https://doi.org/10.1146/annurev-arplant-042916-041124

Tao, H. Y., Xu, S., Tian, Y. C., Li, Z. F., Ge, Y., Zhang, J. P., et al. (2022). Proximal and remote sensing in plant phenomics: 20 years of progress, challenges, and perspectives. Plant Commun. 3, 100344. https://doi.org/10.1016/j.xplc.2022.100344

Atefi, A., Ge, Y. F., Pitla, S., and Schnable, J. (2021). Robotic technologies for high-throughput plant phenotyping: contemporary reviews and future perspectives. Front. Plant Sci. 12. https://doi.org/10.3389/fpls.2021.611940.

Nargesi, M. H., Amiriparian, j., Bagherpour, H., Kheiralipour, K. (2024). Detection of different adulteration in cinnamon powder using hyperspectral imaging and artificial neural network method. 9 (2024*). Results in Chemistry. 9*, 101644.

Nargesi, M.H., Kheiralipour, K. (2024). Ability of visible imaging and machine learning in detection of chickpea flour adulterant in original cinnamon and pepper powders. *Heliyon, 10*(16), e35944.

Farokhzad, S., Modares Motlagh, A., Ahmadi Moghadam, P., Jalali Honarmand, S., Kheiralipour, K. (2024). A machine learning system to identify progress level of dry rot disease in potato tuber based on digital thermal image processing. *Scientific Reports 14* (1), 1995.

Kheiralipour, K., Ahmadi, H., Rajabipour, A., Rafiee, S., Javan-Nikkhah, M., Jayas, D.S. (2013). Development of a new threshold-based classification model for analyzing thermal imaging data to detect fungal infection of pistachio kernel. Agricultural Research, 2, 127-131.

Kheiralipour, K., Pormah, A. (2017). Introducing new shape features for classification of cucumber fruit based on image processing technique and artificial neural networks. J. Food Process Eng. 40, e12558.

Hosainpour, A., Kheiralipour, K., Nadimi, M., Paliwal, J. (2022). Quality assessment of dried white mulberry (*Morus alba* L.) using machine vision. Horticulturae, 8(11), 1011.

Khazaee, Y., Kheiralipour, K., Hosainpour, A., Javadikia, H., Paliwal, J. (2022). Development of a novel image analysis and classification algorithms to separate tubers from clods and stones. *Potato Res., 65*, 1-22.

Illguth, M., Kapteina, G., Kim Soriano, J., Ikeda, Y. (2024). Detection of chlorine in cement matrix using microwave-enhanced laser-induced breakdown spectroscopy. Vol. 32, No. 16 / 29 Jul

2024 / Optics Express 28728. https://doi.org/10.1364/OE.528517.

Kheiralipour, K., Jayas, D.S. (2023a). Advances in image processing applications for assessing leafy materials. *International Journal of Tropical Agriculture. 41*(1-2), 31-47.

Kheiralipour, K., Jayas, D.S. (2023b). Image Processing for the Quality Assessment of Flour and Flour-Based Baked Products. In Image Processing: Advances in Applications and Research. Edited by Jayas, D.S. New York, USA: Nova Science Publishers.

Kheiralipour, K., Singh, C.B., Jayas, D. S. (2023b). Applications of Visible, Thermal, and Hyperspectral Imaging Techniques in the Assessment of Fruits and Vegetables. In: D.S. Jayas. Image Processing: Advances in Applications and Research. Nova Science Publishers, Hauppauge, New York.

Vadivambal, R., and Jayas D.S. (2016). Bio-Imaging: Principles, Techniques, and Applications. 1st Ed, Boca Raton, Florida, USA, CRC Press.